JCTC Journal of Chemical Theory and Computation

Article

pubs.acs.org/JCTC

How Important is Orbital Choice in Single-Determinant Diffusion Quantum Monte Carlo Calculations?

Manolo C. Per,*[,†,‡] Kelly A. Walker,[‡] and Salvy P. Russo[‡]

[†]Virtual Nanoscience Laboratory, CSIRO Materials Science and Engineering, Parkville, VIC 3052, Australia

[‡]Applied Physics, School of Applied Sciences, RMIT University, Melbourne 3001, Australia

ABSTRACT: The accuracy of total electronic energies obtained using the fixed-node diffusion quantum Monte Carlo (FN-DMC) method is determined by the choice of the many-body nodal surface. Here, we perform a systematic comparison of the quality of FN-DMC energies for a selection of atoms and diatomic molecules using nodal surfaces defined by single determinants of Hartree−Fock, B3LYP, and LDA orbitals. Through comparison with experimental results, we show that the use of Kohn−Sham orbitals results in significantly improved FN-DMC atomization energies over those obtained using Hartree−Fock orbitals. We also discuss the effect of spin contamination in the orbitals.

1. INTRODUCTION

The diffusion quantum Monte Carlo (DMC) method is a powerful technique for solving the quantum many-body problem.[1] In the context of electronic structure calculations, DMC offers an interesting alternative to traditional quantum chemistry approaches, scaling as N^3 where N is the number of electrons in the system. The method is relatively simple to implement, and it can take advantage of large computational resources, scaling almost linearly over thousands of processors.

Practical electronic structure DMC calculations use the fixed-node (FN) approximation[2] to address the fermion sign problem. In the FN-DMC approach a trial wave function is used to fix the nodal surface—the $(3N - 1)$-dimensional hypersurface on which the wave function vanishes and across which it changes sign. Importantly, the FN-DMC energy depends only on the shape of the nodal surface. The behavior of the trial wave function away from the nodal surface can influence the stability and efficiency of the calculation, but not the value of the total energy. The FN-DMC ground-state energy is variational, with respect to the shape of the nodal surface, so knowledge of the exact nodal surface is sufficient to obtain the exact ground-state energy. Unfortunately, exact nodal surfaces are known only for extremely simple systems.[3]

Approximate nodal surfaces for many-electron systems can be obtained in a number of ways. The simplest and computationally least expensive approach is to construct a single determinant using the single-particle orbitals obtained from a Hartree−Fock or Kohn−Sham density functional theory calculation. Other approaches, which can increase the accuracy (but also the complexity and cost) of FN-DMC calculations include the use of multiple determinants, backflow transformations,[4] Pfaffians,[5] geminal products,[6] direct optimization of orbitals,[7] and various combinations of these. In this work, we will be concerned exclusively with nodal surfaces obtained from single determinant trial wave functions. While it is known that such simple nodal surfaces are not sufficient for high-quality descriptions of systems containing a large amount of non-dynamical correlation, their relatively low computational cost means they can be used in larger systems.

There are a few results in the literature which hint that single-determinant nodal surfaces built from Kohn−Sham orbitals are superior to those built using Hartree−Fock orbitals. All-electron calculations of the water molecule found that the use of B3LYP orbitals to define the nodal surface led to slightly lower (∼1 kcal/mol) FN-DMC energies than using Hartree−Fock orbitals.[8,9] Wagner and Mitas[10] found a much larger effect in their pseudo-potential studies of transition-metal-oxide molecules, where the use of B3LYP orbitals gave FN-DMC results up to 17 kcal/mol lower in energy than using Hartree−Fock orbitals. It has also been observed that using PBE1w orbitals leads to lower FN-DMC energies than using Hartree−Fock orbitals in solid-state calculations of the B1 AFM-II phase of MnO.[11]

In this paper, we investigate the effect of orbital choice by calculating all-electron FN-DMC energies of the first- and second-row atoms and 15 diatomic molecules, using single-determinant guiding wave functions constructed from Hartree−Fock, B3LYP, and LDA orbitals. We then compare the atomization energies of the molecules with experimental results. Previous benchmark studies of single-determinant FN-DMC atomization energies have been performed at the pseudo-potential[12] and all-electron[13] levels, but neither study included a systematic investigation into the effect of orbital choice.

2. METHODS

2.1. Fixed-node Diffusion Monte Carlo. The diffusion quantum Monte Carlo method is based on the imaginary-time Schrödinger equation, which resembles a classical diffusion equation. The method can be expressed as an integral equation,

$$f(\mathbf{R}', t + \tau) = \int \tilde{G}(\mathbf{R}, \mathbf{R}'; \tau) f(\mathbf{R}, t)\, d\mathbf{R} \quad (1)$$

which describes the evolution of an initial probability distribution $f(\mathbf{R},t)$ under the action of the importance-sampled Green's function, defined as

Received: November 18, 2011
Published: June 13, 2012

ACS Publications © 2012 American Chemical Society

$$\tilde{G}(\mathbf{R}, \mathbf{R}'; \tau) = \Psi_T(\mathbf{R}')\langle \mathbf{R}|e^{-\tau(H-E_T)}|\mathbf{R}'\rangle\Psi_T^{-1}(\mathbf{R}) \quad (2)$$

Here, Ψ_T is a user-defined trial or guiding wave function, H is the Hamiltonian of the system, and E_T is an energy offset. It can be shown[1] that, at long times ($\tau \to \infty$), the initial distribution evolves to become proportional to the product of the exact ground-state wave function and the trial wave function:

$$\lim_{\tau\to\infty} f(\mathbf{R}', t + \tau) \propto \Psi_0(\mathbf{R}')\Psi_T(\mathbf{R}') \quad (3)$$

In order to be able to interpret $f(\mathbf{R})$ as a probability distribution, the trial wave function must have the same sign as the true ground-state wave function over all space. In systems of many indistinguishable fermions, the true ground-state must change sign in order to be antisymmetric and, therefore, must have a nodal surface. The exact structure of this nodal surface generally is unknown. Many-electron DMC calculations use the fixed-node approximation, in which the nodal surface is constrained to be equal to that of the trial wave function, Ψ_T. In this approach, the limiting distribution $f(\mathbf{R}')$ becomes the product of the trial wave function and the lowest-energy wave function compatible with the boundary conditions defined by the fixed nodal surface,

$$\lim_{\tau\to\infty} f(\mathbf{R}', t + \tau) \propto \Psi_0^{\mathrm{FN}}(\mathbf{R}')\Psi_T(\mathbf{R}') \quad (4)$$

The total FN-DMC energy is calculated as an expectation value over this distribution:

$$E_{\text{FN-DMC}} = \frac{\int \Psi_0^{\mathrm{FN}}\Psi_T E_L \, d\mathbf{R}}{\int \Psi_0^{\mathrm{FN}}\Psi_T \, d\mathbf{R}} \quad (5)$$

where the local energy is defined as $E_L = H\Psi_T/\Psi_T$.

In practice, the distribution $f(\mathbf{R})$ is represented by a collection of discrete weighted walkers that evolve stochastically, according to eq 1. The general form of the Green's function is only known in the short-time limit $\tau \to 0$, through a Trotter–Suzuki expansion. To reach the long-time limit, a large number of small-τ steps are taken. This procedure is typically repeated for a number of small values of τ, and the results are extrapolated to obtain the $\tau \to 0$ limit.

All of our QMC calculations were performed using our QuíMiCa code. The FN-DMC algorithm we use is similar to that of Umrigar et al.,[14] which takes into account the behavior of the Green's function near nodes and nuclei. We used a target population of 6400 walkers and time steps of τ = 0.01, 0.005, 0.001 au. An additional time step of τ = 0.0002 au was used for the heaviest systems to ensure that the correct limiting behavior was obtained. The total energies were extrapolated to τ = 0 by fitting a quadratic function to the small-τ results.

2.2. Wave Functions. We use trial wave functions of the Slater–Jastrow form,

$$\Psi_T = D^{\uparrow}D^{\downarrow}\exp(J) \quad (6)$$

where $D^{\uparrow,\downarrow}$ are determinants of spin-up and spin-down single-particle orbitals and the Jastrow term J includes explicit electron correlation terms. The factorization of a single determinant into the product of spin-up and spin-down determinants has no effect on the expectation value of the energy, because the Hamiltonian that we use is spin-independent.

For the purposes of the present study, the most important part of the trial wave function is the choice of orbitals used to construct the Slater determinants, as they determine the nodal surface and, hence, the FN-DMC energy. We use spin-unrestricted orbitals from Hartree–Fock, B3LYP, and LDA calculations performed with the ADF program[15] using the Slater-type QZ4P basis set. This basis has been shown[13] to result in Hartree–Fock basis set errors of <0.1 kcal/mol for the first-row atoms, and <1 kcal/mol for the second-row atoms. The orbitals were cusp-corrected using the method in ref 16 to ensure that the trial wave functions had the correct behavior close to nuclei.

The Jastrow correlation factor contains electron–electron, electron–nucleus, and electron–electron–nucleus terms, and is symmetric with respect to electron exchange. The various correlation terms are written as a power series in the electron–electron and electron–nucleus distances, as described in ref 17. The Jastrow factor does not effect the nodal surface defined by the orbitals in the determinantal part of the trial wave function and, therefore, has no effect on the value of the total FN-DMC energy. It is included to improve the efficiency and stability of the FN-DMC calculation by making the trial wave function a better approximation to the true ground-state wave function. For each system, we optimized separate Jastrow factors for each type of orbital used in the determinant by minimizing the unreweighted variance of the local energy at the variational Monte Carlo level.[18]

3. RESULTS AND DISCUSSION

In order to investigate the effect of orbital choice, we performed FN-DMC total energy calculations on the first- and second-row atoms Li–Ar, and a selection of 15 diatomic molecules. The molecules were fixed at their experimental bond lengths, taken from ref 19.

All FN-DMC results have an associated statistical uncertainty, because of the stochastic nature of the method. These uncertainties were calculated using an approach similar to that described in ref 20, which accounts for the presence of serial correlation in the samples on-the-fly. Statistical uncertainties in the last significant digit (at the level of one standard deviation) are reported in parentheses (for example, 0.04(25) indicates a value of 0.04 ± 0.25).

3.1. DMC Energies. Table 1 lists the FN-DMC total energies obtained using Hartree–Fock (DMC/HF) and Kohn–Sham (DMC/B3LYP and DMC/LDA) orbitals in the Slater determinant. The differences between these FN-DMC energies are shown in Figure 1. The effect of orbital choice on atomic FN-DMC energies is very weak, with the majority of cases being within error bars of showing no orbital dependence at all. The three atoms Al, S, and Ar show a slightly stronger orbital dependence within the resolution of the calculations, but even in these cases, the energy differences are small (~0.5–1 kcal/mol) with relatively large statistical uncertainties (0.35–0.52 kcal/mol).

The FN-DMC energies of molecules show a much stronger dependence on orbital choice than isolated atoms. As shown in Figure 1b, using Kohn–Sham orbitals resulted in lower FN-DMC energies than using Hartree–Fock orbitals for all the molecules that we studied. The DMC/B3LYP and DMC/LDA energies are very similar for most of the molecules. The only significant differences are for ClF and S_2, where the DMC/B3LYP energies are noticeably lower than the DMC/LDA values. In general, the largest improvement over the DMC/HF results occurs in molecules containing first-row atomic species. The most striking results were obtained for CN and F_2, for which the Kohn–Sham nodal surfaces resulted in FN-DMC energies around 14 and 19 kcal/mol lower, respectively, than

Table 1. Total DMC Energies Obtained Using Nodal Surfaces Defined by Hartree-Fock, B3LYP, and LDA Orbitals. All values in Hartree

	Energy (Hartree)		
system	DMC/HF	DMC/B3LYP	DMC/LDA
Li	−7.478028(26)	−7.478045(27)	−7.478055(25)
Be	−14.65751(25)	−14.65723(25)	−14.65728(23)
B	−24.64008(25)	−24.64045(21)	−24.63973(27)
C	−37.83016(27)	−37.83052(21)	−37.82999(24)
N	−54.57627(25)	−54.57672(24)	−54.57623(26)
O	−75.05213(28)	−75.05233(29)	−75.05278(25)
F	−99.71839(31)	−99.71855(27)	−99.71887(31)
Ne	−128.92351(29)	−128.92380(27)	−128.92381(29)
Na	−162.24011(29)	−162.24059(30)	−162.24026(29)
Mg	−200.03315(31)	−200.03297(36)	−200.03316(34)
Al	−242.32350(40)	−242.32241(39)	−242.32261(36)
Si	−289.33059(45)	−289.33081(39)	−289.33073(43)
P	−341.22527(48)	−341.22535(47)	−341.22530(42)
S	−398.06977(54)	−398.07083(47)	−398.06814(50)
Cl	−460.10110(59)	−460.10123(52)	−460.10045(49)
Ar	−527.48570(52)	−527.48868(60)	−527.48626(57)
LiH	−8.070155(90)	−8.07024(13)	−8.07014(23)
OH	−75.72136(30)	−75.72275(34)	−75.72304(31)
CN	−92.66784(53)	−92.68910(49)	−92.69028(65)
CO	−113.29101(56)	−113.29308(52)	−113.29398(47)
N_2	−109.50439(55)	−109.50809(57)	−109.50832(60)
O_2	−150.28484(53)	−150.29116(50)	−150.29140(50)
F_2	−199.45898(60)	−199.48881(54)	−199.48939(54)
CS	−436.16357(66)	−436.16936(62)	−436.16899(59)
SiO	−364.68577(59)	−364.68772(53)	−364.68636(56)
SO	−473.31468(62)	−473.32273(57)	−473.32061(64)
ClF	−559.91255(70)	−559.91830(66)	−559.91437(66)
Si_2	−578.78036(67)	−578.78293(61)	−578.78196(66)
P_2	−682.62864(67)	−682.63150(65)	−682.63034(69)
S_2	−796.29824(83)	−796.30499(76)	−796.30039(79)
Cl_2	−920.29189(77)	−920.29618(71)	−920.29399(72)

the Hartree−Fock nodal surfaces. This is partly due to the large amount of spin contamination in the unrestricted Hartree−Fock orbitals, which is not present in the Kohn−Sham orbitals, and will be discussed more in Section 3.3.

Our calculations of the P_2 molecule show that the DMC/B3LYP and DMC/LDA energies are slightly lower than the DMC/HF result (by 1.80(59) and 1.07(60) kcal/mol, respectively). A benchmark study by Grossman,[12] using pseudo-potentials to describe the core electrons, found a similar effect, with DMC/B3LYP and DMC/LDA energies 1.44(9) and 1.50(9) kcal/mol lower, respectively, than the DMC/HF value.

3.2. Atomization Energies. The differences in the FN-DMC energies reported in Figure 1 are small, compared to the total energies of the atoms and molecules, but large enough to be important when comparing molecular atomization energies with experimental values. The FN-DMC atomization energy (D_e^{DMC}) is defined as the difference between the total energy of a molecule and the energies of its constituent atoms.

Experimental values of the atomization energy include contributions from zero-point energy (ZPE), scalar relativistic (SR), and spin−orbit (SO) effects, which are not present in the FN-DMC calculations. Therefore, we have removed the ZPE, SR, and SO contributions from the experimental values (using the values given in ref 21) to define the modified experimental atomization energy D_e^{exp}.

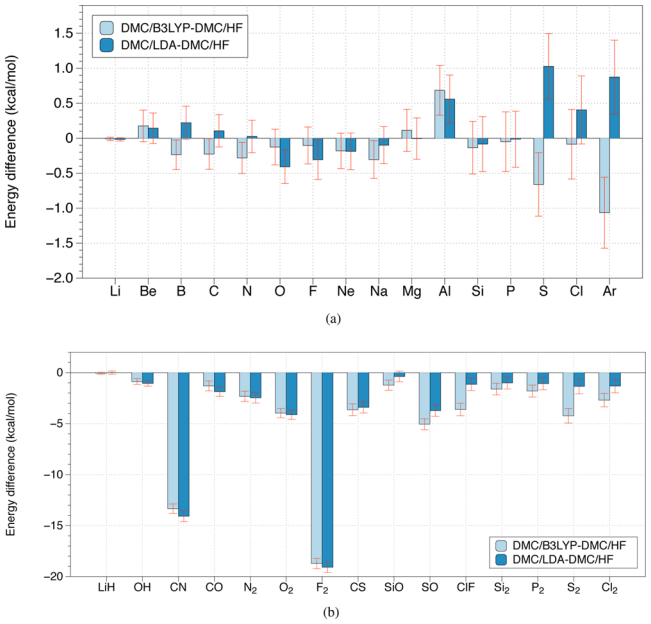

Figure 1. Differences in FN-DMC energies using different orbitals for (a) atoms and (b) molecules. A negative value indicates that the Kohn−Sham nodal surface is superior to the Hartree−Fock nodal surface.

Table 2 reports the differences between D_e^{exp} and the FN-DMC atomization energies obtained using the three different types of orbitals in the trial wave function. The error bars quoted in the table are FN-DMC statistical uncertainties, and they do not include potential uncertainties in the experimental values. The boldface values highlight the most accurate result

Table 2. Systematic Error in the FN-DMC Atomization Energy, Calculated as $D_e^{exp} - D_e^{DMC}$[a]

	Error (kcal/mol)		
system	DMC/HF	DMC/B3LYP	DMC/LDA
LiH	0.190(59)	**0.145(88)**	0.21(15)
OH	0.60(26)	−0.14(28)	**−0.04(25)**
CN	17.86(41)	5.03(37)	**3.65(47)**
CO	3.33(43)	2.38(40)	**1.77(37)**
N_2	7.81(41)	6.06(42)	**5.30(45)**
O_2	7.55(42)	**3.84(41)**	4.25(39)
F_2	25.16(47)	**6.65(41)**	6.69(44)
CS	6.47(57)	3.72(51)	**1.94(52)**
SiO	2.34(50)	**1.37(46)**	2.46(47)
SO	5.14(55)	0.87(50)	**0.79(54)**
ClF	3.20(61)	**−0.22(56)**	1.96(56)
Si_2	**−0.08(58)**	−1.42(52)	−0.92(57)
P_2	5.25(60)	**3.55(59)**	4.21(57)
S_2	3.48(71)	0.57(64)	**0.08(67)**
Cl_2	2.70(72)	**0.17(65)**	0.57(0.63)
MAD (All)	6.07	2.40	**2.32**
MAD (first row)	8.93	3.46	**3.12**
MAD (mixed first and second row)	4.28	**1.54**	1.78
MAD (second row)	2.87	**1.42**	1.44

[a]The smallest error achieved for each system is highlighted in bold.

dx.doi.org/10.1021/ct200828s | J. Chem. Theory Comput. 2012, 8, 2255−2259

for each system. It can be clearly seen that the best results are obtained using the Kohn–Sham nodal surfaces. The one exception is the Si_2 molecule, for which the Hartree–Fock nodal surface gives the most accurate atomization energy, being exact within error bars. It should be noted, however, that the DMC/LDA result for this system is also within two standard deviations of the exact result. The most accurate atomization energies are fairly evenly divided between the DMC/B3LYP and DMC/LDA results, with no definite trend showing definitively better performance for one kind of Kohn–Sham orbital over the other. We obtained surprisingly accurate results for the S_2 and Cl_2 molecules, for which both the DMC/B3LYP and DMC/LDA atomization energies are within error bars of the exact values.

The similar performance of DMC/B3LYP and DMC/LDA is reflected in the mean absolute deviations (MADs) from experiment, which are also listed in Table 2. We report four different MADs: one for all molecules, one for molecules containing only first-row elements, one for molecules containing a mixture of first and second-row elements, and one for molecules containing only second-row elements. The atomization energies obtained using Kohn–Sham nodal surfaces are significantly better than those obtained with Hartree–Fock nodes in all four cases. The DMC/B3LYP and DMC/LDA results have similar MADs in all four cases. For all three types of nodal surfaces considered, the largest MAD is obtained for first-row molecules. This is presumably due to a better cancellation of errors in the core regions of the heavier atoms, which agrees with the observations of Nemec et al.[13]

Using the DMC/HF approach, the largest deviations from experiment were obtained for F_2, CN, and N_2. We have already pointed out that the especially poor results for F_2 and CN are partly due to spin contamination in the unrestricted Hartree–Fock wave function. The two largest deviations obtained using DMC/B3LYP and DMC/LDA are for F_2 and N_2.

3.3. Spin Contamination. The use of spin-unrestricted orbitals in Hartree–Fock and Kohn–Sham calculations gives the greatest variational flexibility to the orbitals, but introduces the possibility of spin contamination. With the exception of F_2 and CN, all of the systems we considered showed little spin contamination. The CN molecule has a large amount of spin contamination at the Hartree–Fock level, but relatively little at the B3LYP and LDA levels. The exact expectation value of the S^2 operator for a system in a doublet state is 0.75. We obtained values of 1.161, 0.759, and 0.755 from Hartree–Fock, B3LYP, and LDA calculations, respectively. The F_2 molecule also suffers from spin contamination at the unrestricted Hartree–Fock level. We obtain $S^2 = 0.358$, in close agreement with ref 22. Our B3LYP and LDA calculations of F_2 produced pure singlet states.

In order to understand to what extent spin contamination was responsible for the large error in the DMC/HF atomization energies of F_2 and CN, we also performed FN-DMC calculations using spin-restricted orbitals. For F_2, these orbitals were generated with ADF, while for CN, we used GAMESS[23] to generate restricted-spin open-shell orbitals, as the version of the ADF code we used (2010.01) only supports unrestricted orbitals for open-shell systems. We used the augmented triple-ζ atomic natural orbital (ANO-TZ) Gaussian-type basis set[24] in the GAMESS calculations, which includes a number of high-exponent basis functions to improve the description of atomic core regions. As an indication of the quality of this basis set, we note that the unrestricted Hartree–Fock energy of CN obtained using the ANO-TZ basis set and GAMESS was only 0.04 kcal/mol higher than the result obtained using the Slater-type QZ4P basis set and ADF.

The smaller amount of variational freedom in the spin-restricted orbitals is evident in the Hartree–Fock energies, which are 6.12 and 10.92 kcal/mol higher than the UHF energies for F_2 and CN, respectively. Despite this, the lack of any spin contamination in these orbitals leads to DMC/RHF energies which are 12.13 and 7.62 kcal/mol *lower* than the DMC/HF results. Consequently, the DMC/RHF atomization energies of F_2 and CN are 13.03(43) and 10.24(37) kcal/mol higher than the experimental values, respectively. Although these are still comparatively large errors, they are substantially smaller than the errors obtained using spin-unrestricted Hartree–Fock orbitals (listed in Table 2). It should be noted, however, that these DMC/RHF results are still significantly worse than those obtained using Kohn–Sham orbitals.

We also investigated the effect of replacing the unrestricted-spin Kohn–Sham orbitals, which displayed little spin contamination, with their restricted-spin open shell equivalents in FN-DMC calculations of CN. This resulted in no significant change in the DMC/B3LYP energy, and an *increase* of 1.59(52) kcal/mol in the DMC/LDA energy.

3.4. Stretched Bonds. Nodal surfaces obtained from single determinant trial wave functions are reasonably accurate at equilibrium geometries, but stretched molecular bonds introduce more-complicated correlation effects,[25] and a multi-determinant description of the nodal surface frequently becomes necessary. Nevertheless, it is interesting to consider the performance of single-determinant nodal surfaces in this situation. To this end, we performed FN-DMC calculations of the binding energy of the F_2 molecule at various stretched bond lengths using spin-unrestricted Hartree–Fock, B3LYP, and LDA nodal surfaces. Spin unrestricted orbitals are used here to give a reasonable description of the dissociation of the singlet-state F_2 molecule into two doublet-state F atoms.

The resulting binding energy curves are shown in Figure 2, where they can be compared with the accurate auxiliary-field quantum Monte Carlo (AFQMC) results from ref 22. The DMC/B3LYP and DMC/LDA results are very similar at each of the bond lengths considered. The error in the atomization energy increases at intermediate bond lengths, consistent with the expected increase in correlation effects in this region. The

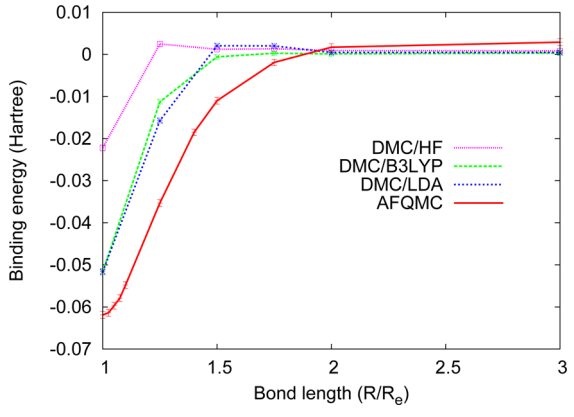

Figure 2. Binding energy of the stretched F_2 molecule from FN-DMC calculations using different nodal surfaces. R_e denotes the experimental equilibrium bond length. Auxiliary-field quantum Monte Carlo (AFQMC) results are taken from ref 22.

poor quality of the DMC/HF results already observed at the equilibrium geometry persists to intermediate bond lengths, where the error in the atomization energy is still nearly twice that obtained with Kohn–Sham nodes at $1.25R_e$.

4. CONCLUSION

In this work, we have investigated the effect of orbital choice on FN-DMC energies using single-determinant trial wave functions to define the many-electron nodal surface. We compared the total FN-DMC energies of first-row atoms, second-row atoms, and a selection of 15 diatomic molecules using trial wave functions constructed from Hartree–Fock, B3LYP, and LDA orbitals.

We found that the FN-DMC energies of isolated atoms are relatively insensitive to orbital choice. Molecular energies show a stronger orbital dependence, with the use of Kohn–Sham orbitals leading to lower FN-DMC energies than using Hartree–Fock orbitals. Therefore, the energy-optimal single-determinant orbitals (i.e., Hartree–Fock) do not correspond to the energy-optimal single-determinant nodal surface. Interestingly, we observed that the use of B3LYP and LDA orbitals led to similar total FN-DMC energies. It appears that the inclusion of some description of electron correlation in the calculation of the single-particle orbitals has a beneficial effect on the many-body nodal surface.

The lower molecular energies obtained using the Kohn–Sham orbitals are reflected in a comparison of the FN-DMC atomization energies with experimental values. Our calculations show that using Kohn–Sham orbitals leads to a mean absolute deviation from experimental atomization energies which is less than half that obtained using Hartree–Fock orbitals (2.32 kcal/mol vs 6.07 kcal/mol). Calculations of the binding energy of the F_2 molecule indicate that Kohn–Sham orbitals continue to provide superior nodal surfaces to Hartree–Fock orbitals as the molecular bond is stretched and correlation effects become even stronger.

We have also found that spin contamination at the unrestricted Hartree–Fock level can have a strong adverse effect on the quality of the nodal surface. Avoiding this contamination by using restricted-spin orbitals does improve the nodal surfaces, but not to the extent that using Kohn–Sham orbitals does.

In conclusion, our results suggest that unrestricted Kohn–Sham orbitals are to be preferred over Hartree–Fock orbitals in the construction of single-determinant trial wave functions for FN-DMC calculations.

AUTHOR INFORMATION

Corresponding Author

*E-mail: manolo.per@csiro.au.

Notes

The authors declare no competing financial interest.

ACKNOWLEDGMENTS

We thank the Victorian Life Sciences Computation Initiative (VLSCI) and the Australian National Computational Infrastructure (NCI) for generous allocations of computer time.

REFERENCES

(1) Foulkes, W. M. C.; Mitas, L.; Needs, R. J.; Rajagopal, G. *Rev. Mod. Phys.* **2001**, *73*, 33–83.
(2) Anderson, J. B. *J. Chem. Phys.* **1976**, *65*, 4121–4127.
(3) Bressanini, D.; Ceperley, D. M.; Reynolds, P. J. In *Recent Advances in Quantum Monte Carlo Methods, II*; Rothstein, S., Ed.; World Scientific: Singapore, 2001; pp 3–11.
(4) López Ríos, P.; Ma, A.; Drummond, N. D.; Towler, M. D.; Needs, R. J. *Phys. Rev. E* **2006**, *74*, 066701.
(5) Bajdich, M.; Mitas, L.; Drobný, G.; Wagner, L. K.; Schmidt, K. E. *Phys. Rev. Lett.* **2006**, *96*, 130201.
(6) Casula, M.; Sorella, S. *J. Chem. Phys.* **2003**, *119*, 6500–6511.
(7) Toulouse, J.; Umrigar, C. J. *J. Chem. Phys.* **2008**, *128*, 174101.
(8) Gurtubay, I. G.; Needs, R. J. *J. Chem. Phys.* **2007**, *127*, 124306.
(9) Benedek, N. A.; Snook, I. K.; Towler, M. D.; Needs, R. J. *J. Chem. Phys.* **2006**, *125*, 104302.
(10) Wagner, L. K.; Mitas, L. *J. Chem. Phys.* **2007**, *126*, 034105.
(11) Kolorenč, J.; Hu, S.; Mitas, L. *Phys. Rev. B* **2010**, *82*, 115108.
(12) Grossman, J. C. *J. Chem. Phys.* **2002**, *117*, 1434–1440.
(13) Nemec, N.; Towler, M. D.; Needs, R. J. *J. Chem. Phys.* **2010**, *132*, 034111.
(14) Umrigar, C. J.; Nightingale, M. P.; Runge, K. J. *J. Chem. Phys.* **1993**, *99*, 2865–2890.
(15) Te Velde, G.; Bickelhaupt, F. M.; Baerends, E. J.; van Gisbergen, S. J. A.; Snijders, J. G.; Ziegler, T.; Fonseca Guerra, C. *J. Comput. Chem.* **2001**, *22*, 931–967.
(16) Per, M. C.; Russo, S. P.; Snook, I. K. *J. Chem. Phys.* **2008**, *128*, 114106.
(17) Drummond, N. D.; Towler, M. D.; Needs, R. J. *Phys. Rev. B* **2004**, *70*, 235119.
(18) Umrigar, C. J.; Wilson, K.; Wilkins, J. *Phys. Rev. Lett.* **1988**, *60*, 1719–1722.
(19) Feller, D.; Peterson, K. A.; Dixon, D. A. *J. Chem. Phys.* **2008**, *129*, 204105.
(20) Kent, D. R., IV; Muller, R. P.; Anderson, A. G.; Goddard, W. A., III; Feldmann, M. T. *J. Comput. Chem.* **2007**, *28*, 2309–2316.
(21) Feller, D.; Peterson, K. A. *J. Chem. Phys.* **1999**, *110*, 8384–8396.
(22) Purwanto, W.; Al-Saidi, W. A.; Krakauer, H.; Zhang, S. *J. Chem. Phys.* **2008**, *128*, 114309.
(23) Schmidt, M. W.; Baldridge, K. K.; Boatz, J. A.; Elbert, S. T.; Gordon, M. S.; Jensen, J. H.; Koseki, S.; Matsunaga, N.; Nguyen, K. A.; Su, S.; Windus, T. L.; Dupuis, M.; Montgomery, J. A. *J. Comput. Chem.* **1993**, *14*, 1347–1363.
(24) Widmark, P. O.; Malmqvist, P. A.; Roos, B. O. *Theor. Chim. Acta* **1990**, *77*, 291–306.
(25) Per, M. C.; Russo, S. P.; Snook, I. K. *J. Chem. Phys.* **2009**, *130*, 134103.